CROATICA CHEMICA ACTA CCACAA **73** (3) 667–704 (2000)

ISSN-0011-1643
CCA-2675

Original Scientific Paper

A Comparative Study of Lead Oxide Modified Graphite Paste Electrodes and Solid Graphite Electrodes with Mechanically Immobilized Lead Oxides

Nina Zakharchuk, Stefan Meyer,** Britta Lange, and Fritz Scholz****

Institut für Chemie und Biochemie, Ernst-Moritz-Arndt-Universität Greifswald, Soldmannstraße 23, D-17487 Greifswald, Germany

Received July 6, 1999; revised February 24, 2000; accepted March 7, 2000

The cyclic voltammetry of red PbO, α-PbO_2, β-PbO_2 and $BaPbO_3$ was studied with two different types of electrodes in acidic and alkaline media. In one case, microcrystalline particles of lead oxides were mechanically immobilized on the surface of paraffin-impregnated graphite rod electrodes (PIGE), while in the other case, lead oxides were added to a paste of graphite and silicone oil. The overall behaviour of lead oxides in both electrodes is very similar to the well-known behaviour of electrodes made of lead oxide powders. The results show that the binder does not effect the overall electrochemistry of lead oxides. Moreover, the electrochemical reactions are more reversible for the paste electrode than in the case of the PIGE.

Key words: mechanical immobilization, modified graphite paste electrode, cyclic voltammetry, lead oxides.

INTRODUCTION

Numerous publications demonstrate the widespread applicability of the mechanical attachment of a solid compound to the surface of a suitable solid

* Permanent address: Institute of Inorganic Chemistry, Siberian Branch of Russian Academy of Science, Ac. Lavrentyev pr. 3, 630090 Novosibirsk, Russia.

** Current address: MTU Motoren und Turbinen-Union, München GmbH, Dachauer Straße 665, 80995 München, Germany.

*** Author to whom correspondence should be addressed. (E-mail: fscholz@rz.uni-greifswald.de)

electrode (abrasive transfer technique)[1–9] and modified graphite paste electrodes[10–20] in the field of electrochemical analysis,[10] for the solution of some physicochemical problems[16–20] and for studying the electrochemistry of compounds which can be synthesized in large quantities and therefore can easily be characterized by other analytical or physical methods.[1–9,14,15] Such characterisation cannot always be done when the compounds are synthesized as thin films on solid electrode surfaces. The electrochemical behaviour of solids at the surface of these two kinds of electrodes may be either identical or significantly different. In the first case, the solid is transferred onto the electrode surface by using mechanical immobilization.[1–3] Even if the substance is very carefully prepared, it will be unevenly distributed on the electrode surface in the form of separate agglomerates. In the second case, the substance is introduced into the volume of the graphite paste electrode by evenly distributing the particles in the graphite paste. Because of the roughness of this electrode, the electrode reaction can to some extent proceed into the paste and larger amounts of substance can be involved. The second reason for differing results may be the presence of oil in the graphite paste as a binder between the graphite and sample particles. The oil of the paste electrodes may inhibit the electrochemical reactions, leading to a certain additional overpotentional of reactions. Recently,[21] we have shown that the overall behaviour of Prussian blue in both electrodes is very similar to the well-known behaviour of electrodes with an electrochemically synthesized Prussian blue film. Nevertheless, the binder affects the electrochemistry of Prussian blue to a certain extent. Differences have been observed for the modified paste electrode, particularly in acidic solutions. It is interesting to perform such comparative studies with other solids, for example, with oxide compounds as their electrochemistry has been sufficiently studied with graphite paste electrodes.[10–12,22,23]

Here, the possibilities of both electrodes for the study of the behaviour of red PbO, α-PbO_2, β-PbO_2, and $BaPbO_3$ in acidic and alkaline media are examined. These studies are a necessary step towards electrochemically investigating phase stability, determining the degree of the oxidation of elements and assessing the electronic properties of such phases as, for example, $Bi_{2-x}Pb_xSr_2Ca_2CuO_{8+\delta}$,[18] $Bi_{2-x}Pb_xBaLaCuO_{6+\delta}$[20] and other cuprates. Literature data on the electrochemical behaviour of PbO are rather rare while the standard potentials of several different oxides are available.[24] Without referring to other sources, Brainina and coauthors[11] wrote that the oxidation of yellow PbO proceeds at +0.6 V whereas the oxidation of red PbO does so only at +1.2 V in 0.1 M NaOH solution. They suggested using this effect for the identification of these phases in mixtures. Other authors[23] studied the electrochemical behaviour of PbO and PbO_2 in graphite paste electrodes prepared from graphite powder and where the aqueous electrolyte 0.1 M

NaOH was used as a binder. Unfortunately, the authors[23] did not mention which modifications of lead oxides have been studied. There are many data about the electrochemistry of both modifications of lead dioxide in strongly alkaline and sulfuric acid solutions[29,30] and of α-PbO_2 in neutral media.[31] No data on the electrochemical behaviour of $BaPbO_3$ are available.

EXPERIMENTAL

Equipment

All measurements were made with an Autolab (ECO-Chemie, Utrecht, Netherlands), an electrode stand VA 633 (Metrohm, Herisau, Switzerland), and a 386 personal computer. The reference electrode (Metrohm, Switzerland) was an Ag/AgCl electrode with 3 mol l^{-1} KCl (E = 0.208 V *vs*. SHE). All measurements were performed in solutions, which were thoroughly deaerated with high-purity nitrogen for at least 10 min. The voltammograms were recorded at 22 ± 1 °C.

Chemicals

$BaPbO_3$ was prepared from high-purity powders of $BaCO_3$ and PbO_2 by conventional solid state procedure. Temperatures of 500–780 °C were used for the thermotreatment of compressed tablets. Subsequent annealing was accomplished within a range of 530–1120 °C. The phase purity of $BaPbO_3$ was controlled by X-ray analysis (Philips APD 1700, Cu-Kα radiation). The data obtained by a full chemical analysis of samples showed this phase to have a barium deficit, and the composition of the phase was found to be $Ba_{0.80\pm0.03}PbO_{3.10\pm0.02}$. The structure is of rhombic perovskite type having the following unit cell parameters: a = 6.024, b = 6.065 and c = 8.506 Å. β-PbO_2 and α-PbO_2 were prepared according to what has been described in Ref. 29, p. 681, and in Ref. 32, respectively. X-ray diffraction pattern showed that the synthesized samples are single-phase systems. The following chemicals (Merck) were used: yellow and red PbO, Pb_3O_4, $NaClO_3$, $NaNO_3$ and HNO_3. The electrolyte solutions were prepared from HCl (Merck, analytical grade) and KOH (Merck, analytical grade) using twice distilled ion-exchanged water. The graphite paste electrodes were made from graphite powder (Merck, Germany) and silicone oil (NM 500, Nünchritz, Germany).

Electrode Preparation

Abrasive Transfer Technique

A few milligrams of the solid compound were placed on a spot on a clean glazed porcelain tile. The lower circular surface of a paraffin-impregnated graphite rod electrode (PIGE) was gently rubbed on the compound spot to transfer the sample onto the electrode surface. The PIGEs were made by impregnating graphite rods with melted paraffin (m.p. 65 °C) under vacuum. The graphite rods were the usual type of electrodes for spectrometric emission analysis with a diameter of 5 mm. Detailed descriptions of PIGEs and the abrasive transfer technique are published elsewhere. [1]

Modified Graphite Paste Electrodes

The finely powdered solid compound was mixed with graphite powder in a ratio of (5×10^{-5} to 5×10^{-4}) mol to 1 g graphite paste. This powder mixture was transferred to an agate mortar and mixed thoroughly for 1–2 min with 2–3% (mass fractions, w) of silicone oil. The homogeneous paste was filled into the electrode holder, which was an impregnated graphite rod enclosed in a Teflon tube several millimetres longer than the rod and forming a cup. The cup was filled with the paste, and the electrode surface was smoothed on the flat surface of a glazed tile or a glass plate. The diameter of the electrode surface was 5 mm. A suitable check of the homogeneity of the paste was the reproducibility of the peak currents obtained for a number of renewed electrodes.

RESULTS AND DISCUSSIONS

The background current of a graphite paste electrode and a PIGE in contact with 0.1 M HCl and 1 M NaOH exhibits some differences (see also Ref. 21). The cathodic range of the paste electrode is smaller in acid solution while the anodic range is smaller in alkaline solutions. Probably, the simple reason is that the true surface area of the paste electrode is much larger because of its roughness. The currents are equivalent in the potential range from 0.9 to –1.0 V for 0.1 M HCl and from 0.5 to –1.2 V for 1 M NaOH.

The Electrochemical Behaviour of Lead Oxides in Contact with a Hydrochloric Acid Electrolyte

In the synthesis of several copper-bismuth high-temperature superconductors, lead oxides are added to stabilize the structure. In combination with other physical and physicochemical methods, solid state voltammetry can help to elucidate the role of lead in the formation of the high-temperature superconducting phase. Thus, the questions arises what is the limit of solubility of lead oxides in the system and what is the oxidation state of lead in this phase. These problems have been studied for copper and bismuth in 123, 2201 and 2221 phases.[16–20] From the specific composition of the copper and bismuth containing ceramics, it follows that the most suitable electrolyte is a weakly acidic solution of hydrochloric acid. For these studies, it is very important to know the voltammetric behaviour of the pure phases that constitute the complex system. Unfortunately, there are only insufficient literature data available concerning the linear sweep voltammetry of lead oxides with hydrochloric acid solutions as electrolyte.

Red PbO

From a thermodynamic point of view[24–28] in acidic electrolytes, the reduction of PbO can be described as

$$PbO_{red} + 2H^+ + 2e^- = Pb^o + H_2O$$
$$E^o = +\,0.040\ \text{V}\ \textit{vs.}\ \text{Ag/AgCl} \qquad (1)$$

At pH = 1, the formal potential of this reaction is –0.019 V *vs.* Ag/AgCl. Figure 1 shows typical cyclic voltammograms of red PbO at the PIGE and at the paste electrode in 0.1 M HCl. The reduction of PbO proceeds at one single peak C at the paste electrode. At the PIGE, the signal of PbO reduction exhibits a more complicate form and is less reproducible. As a rule, one observes at the descending part of the peak a shoulder (Figure 1b) or a second peak C_2 (Figure 1a, dark line). The potential of peak C ($E_{p(C)}$) depends on the charge that is consumed during reduction. Figure 2a shows that $E_{p(C)}$ shifts from –(0.630 ± 0.02) V to –(0.680 ± 0.01) V for the paste electrode and from –(0.680 ± 0.04) to –(0.730 ± 0.03) V for the PIGE, when the charge increases from 0.1 to 1.2 mC. The slope of the dependence of $E_{p(C)}$ on Q is the

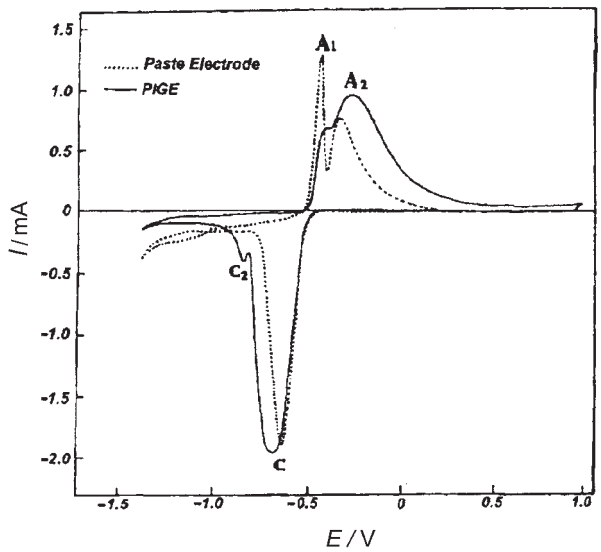

Figure 1. Typical cyclic voltammograms of red PbO dispersed in the graphite paste electrode and immobilized at the PIGE surface. Scan rate: 100 mV s^{-1}; electrolyte: 0.1 M HCl; starting potential: 1.0 V.

same for the paste electrode as for the PIGE, but the absolute values are about 50 mV more negative for the PIGE (Figure 2a). The peaks are also much broader on the PIGE especially for charges above 4.5 mC (Figure 2b). In both cases the dependence of the half-width of the peak on Q exhibits two parts with different slopes. This indicates that the mechanism changes with increasing charge, *i.e.* with an increasing amount of reacting PbO. For the PIGE and the graphite paste electrode, the reduction appears at more negative potentials as compared to the formal potential of reaction (1). This shift of the reduction is not only due to a mass-transport effect but it is certainly also the result of irreversibility. Two anodic signals (A_1 and A_2) appear in the cyclic voltammograms for the dissolution of elementary lead. They are observed at both electrodes. No response indicating a subsequent oxidation of Pb^{2+} to Pb^{4+} is observed.

Until now there are no mathematical models available which sufficiently describe the electrochemical conversions of solid compounds. Only limited features of the electrochemical processes can be studied so far. Thus, it

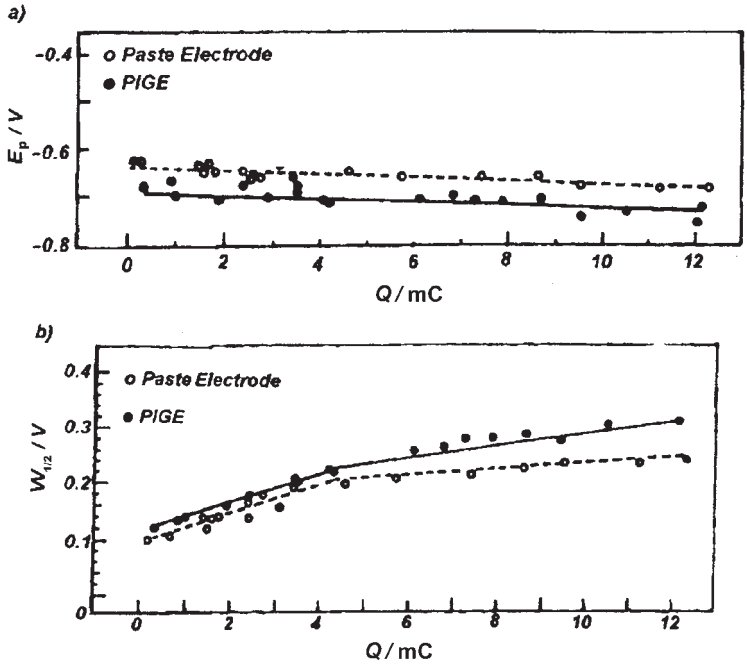

Figure 2. Plot of (a) potential and (b) half-width of peak C *versus* the amount of charge consumed during reduction of PbO dispersed in the graphite paste electrode (–○–) and immobilized on the PIGE (–●–). Conditions as in Figure 1.

is possible to estimate the role of diffusion in electrochemical processes by measuring the dependence[33] of the peak current on the scan rate v. Under certain conditions, information can be obtained from plots of peak currents (I_p) and peak potentials (E_p) *versus* the logarithm of the scan rate, which says whether there are parallel or follow-up reactions present, and it is possible to determine the effective transfer coefficients[10–12] αn and βn. Figures

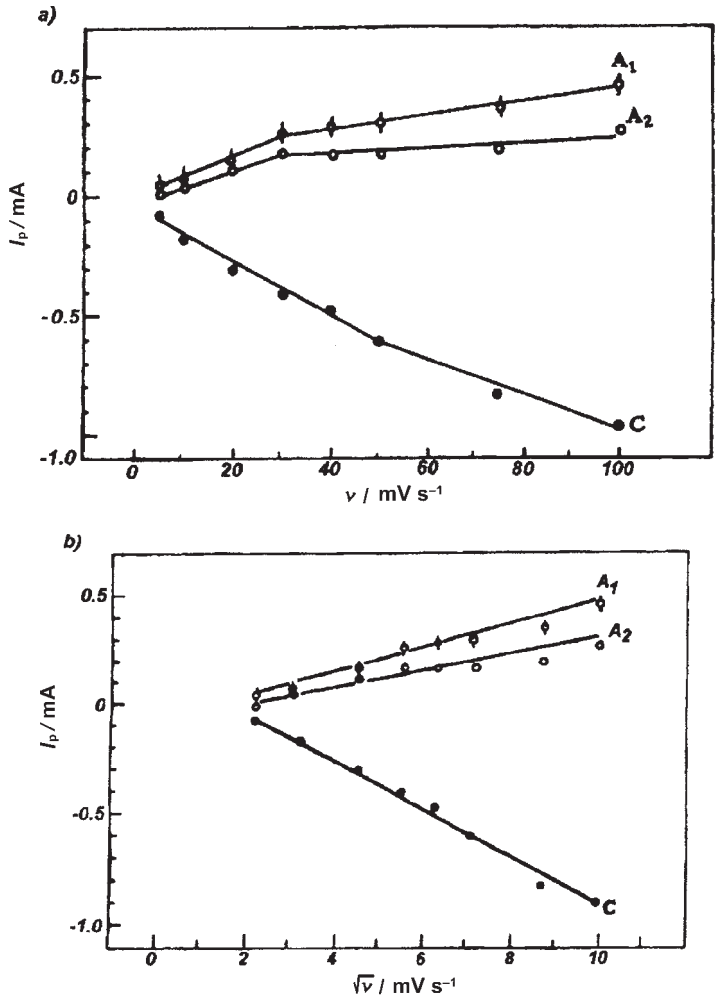

Figure 3. Plot of peak currents of C, A1 and A_2 *versus* scan rate (a), and *versus* square root of the scan rate (b) for electrochemical conversions of PbO dispersed in the graphite paste electrode. Electrolyte: 0.1 M HCl; concentration of PbO in the graphite paste: 5×10^{-5} mol g^{-1}; starting potential: 1.0 V.

3 and 4 show such plots for the peaks C, A_1 and A_2 at the graphite paste electrode. The linear dependence of the peak current on the square root of the scan rate (Figure 3) indicates a diffusion character of the observed signals. The fact that two linear parts are present in the plot of $E_{p(C)}$ *vs.* the log ν with slopes of 60 mV and 120 mV, resp., indicates the presence of two competing electrode reactions (Figure 4a, curve C). Based on the equations $dE_p / d\lg \nu = 0.059 / \alpha n$ (or βn),[11] the effective transfer coefficients can be cal-

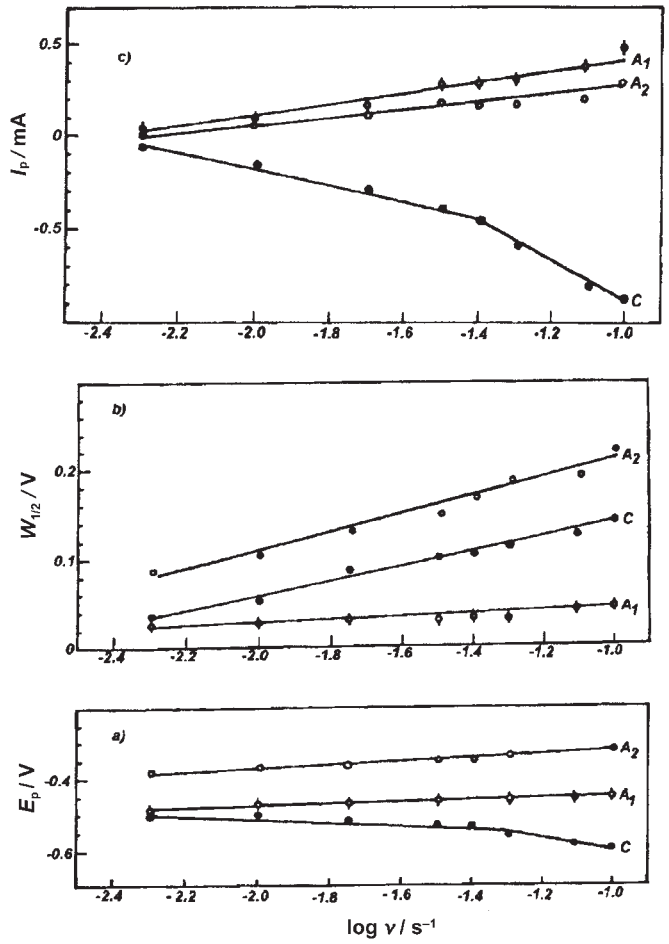

Figure 4. Plot of (a) peak potentials, (b) half-width, and (c) peak currents of peaks C, A_1 and A_2 *versus* logarithm of scan rate for the electrochemical conversions of PbO dispersed in the graphite paste electrode. Electrolyte: 0.1 M HCl; concentration of PbO in the graphite paste: 5×10^{-5} mol g^{-1}; starting potential: 1.0 V. On top is given the plot of peak currents *versus* logarithm of scan rate.

culated for the cathodic and the anodic processes. With respect to curve C, the effective transfer coefficient for the first step of the PbO reduction is near to 1 for scan rates below 50 mV s^{-1}. For scan rates above 50 mV s^{-1}, signal C is due to another reaction for which the effective coefficient is 0.5. Based on these results, we suggest that reaction (1) is accompanied by the following reactions:

$$PbO_{red} + 2H^+ \rightarrow Pb^{2+}{}_{(gr.)} + H_2O \quad (2)$$

and

$$Pb^{2+}{}_{(gr.)} + 2e^- \rightarrow Pb^{o}{}_{(gr.)}$$
$$E^\circ = -0.334 \text{ V } (vs. \text{ Ag/AgCl})\ ^{24} \quad (3)$$

((gr.) indicates that the species is confined to the graphite surface).

Reaction (3) occurs at the graphite/electrolyte interface, whereas the reaction (1) occurs in the solid phase and may be written as:

$$PbO + 2H^+{}_{(PbO)} + 2e^- = Pb^{o}{}_{(PbO)} + H_2O \quad (4)$$

(The subscript (PbO) indicates the locus of the species).

Obviously, this reaction is slow and determines the electrochemical reduction of PbO in the presence of weakly acid solutions. Therefore, the half-width $W_{1/2}$ of peak C will increase by more than 100 mV, if the scan rate increases from 5 to 100 mV s^{-1} (Figure 4b, curve C). With this interpretation one can well understand that the electrochemical dissolution of elementary lead proceeds along two different pathways:

$Pb^{o}{}_{(gr.)} = Pb^{2+} + 2e^-$ (peaks A_1) and $Pb^{o}{}_{(PbO)} = Pb^{2+} + 2e^-$ (peak A_2).

In both cases, elementary lead in its stable cubic modification is dissolved in the electrode process. In a previous *in-situ* X-ray electrochemical study,[34] it has been shown that cubic lead is formed in a topotactic solid-state electrochemical reduction of PbO. Peak A_1 is identical with the anodic dissolution peak of lead after preliminary cathodic plating from a Pb^{2+} solution. The reason for the appearance of peak A_2 at potentials which are more positive than those of A_1 can be as follows: Pb which is formed in a topotactic solid-state electrochemical reduction of PbO will be situated at such places where the PbO was present, and it might not be as well-crystallized as that deposited from solution. Pb that has been plated from a solution will be situated at the most active centres of the graphite surface, and it will be more ideally crystallized. This makes it understandable that the resistance of the lead-graphite interface can differ remarkably. The resistance of the

interface will be higher for the lead formed from PbO and it will be smaller or even negligible for the lead deposited from a solution. This model is consistent with the behaviour of the voltammetric peaks. Peak A_2 is very broad and is situated at more positive potentials. E_p and $W_{1/2}$ of A_1 and A_2 depend linearly on the scan rate (Figure 4, curves A_1 and A_2). All parameters of peak A_1 are similar to the stripping peak for the reversible reaction: $Pb^{2+} + 2e^- \leftrightarrow Pb^o$ at impregnated graphite electrodes.[10–12] For this peak, the slope of $E_p = f(\log v)$ is 26 mV (Figure 4a, curve A_1). The half-width of the peak slightly changes with the scan rate and it never exceeds 45 mV (Figure 4b, curve A_1). In case of A_2, there arises the question why the slope of $E_p = f(\log v)$ is only 56 mV although the peak is so broad (Figure 4b, curve A_2). Peak A_2 is more pronounced when the PbO is mechanically attached to a PIGE than in the case of its incorporation in a graphite paste electrode (Figure 1a, dark curve, and 1b). We suppose that the chemical reaction is faster at the PIGE than at the paste electrode. Additionally, the adsorption capacity of the PIGE is smaller than that of the paste electrode. At the PIGE, the dissolved Pb^{2+} ions can easily escape the reaction (3) by diffusion. Then the reaction (4) will dominate. As the PbO is present at the PIGE in the form of larger agglomerates of particles, the ohmic resistance at the graphite-lead interface may also exceed the one in the case of paste electrodes.

α-PbO₂ and β-PbO₂

For the following electrochemical reactions of PbO_2, the respective thermodynamic data[24–29] are presented:

$$PbO_2 + 2H^+ + 2e^- \rightarrow Pb^{2+} + 2OH^-$$
$$E_f = 1.747 - 0.059 \log a_{OH^-} - 0.0295 \log a_{Pb^{2+}} \quad (5)$$

$$3PbO_2 + 4H^+ + 4e^- \rightarrow Pb_3O_4 + 2H_2O$$
$$E_f = 1.014 - 0.059\ pH \quad (6)$$

$$PbO_2 + 2H^+ + 2e^- \rightarrow PbO + H_2O$$
$$E_f = 0.899 - 0.059\ pH \quad (7)$$

$$PbO_2 + H_2O + 2e^- \rightarrow PbO + 2OH^-$$
$$E_f = 0.040 - 0.059 \log a_{OH^-} \quad (8)$$

$$PbO_2 + 4H^+ + 4e^- \rightarrow Pb^o + 2H_2O$$
$$E_f = 0.458 - 0.059\ pH \quad (9)$$

At pH = 1, the formal potentials of these reactions are 1.747 – 0.0295 $\log a_{Pb^{2+}}$, 0.955, 0.840, 0.807 and 0.399 V, respectively.

Reactions (7) and (8) belong to the same reaction, the one formulated for an acidic solution and the other for an alkaline solution, but for a certain pH the formal potentials of both reactions must be identical. The difference of 33 mV in the formal potentials is due to different literature sources.

Figure 5 shows the cyclic voltammograms of the electrochemical conversion of α- and β-PbO_2 at the graphite paste electrode and at the PIGE using 0.1 M HCl as electrolyte. The voltammograms were recorded in the potential range from 1.4 to –1.5 V at a scan rate of 100 mV s^{-1}. From this figure, it follows that both modifications can be reduced in consecutive steps to Pb^{2+} and Pb^o :

$$Pb^{4+} + 2e^- \rightarrow Pb^{2+}\ (\text{peak } C_1) + 2e^- \rightarrow$$
$$Pb^o\ (\text{peak } C_2) - e^- \rightarrow Pb^{2+}\ (\text{peak A}) \quad (10)$$

For both electrodes, the potentials of the first signal (peak C_1) are identical and they are determined only by the structure of PbO_2. For the orthorhombic α-PbO_2, the potential of peak C_1 is about 50 mV more positive than for the tetragonal β-PbO_2 (Figures 5a and 5b). The standard potential of the α-PbO_2 electrode is only 7–8 mV more positive than that of the β-PbO_2 electrode in sulfuric acid solution.[29] With an increasing amount of consumed electric charge, the potential of peak C_1 shifts only slightly by 2.5 mV/mC (Figure 6a). The peak potential fluctuates betwen + 0.95 and + 0.85 V, depending on the modification of PbO_2 and also depending on the amounts of substance on the electrode surface. A comparison of these potentials with the formal potentials of reactions (5) to (9) shows that these processes may be involved in peak C_1. The question which of these reactions is of main significance has to be studied in further experiments.

We propose that in weakly hydrochloric acid both hydrogen ions and water molecules participate in the electrode process with the generation of both Pb^{2+} ions and PbO or Pb_3O_4 in the pre-electrode layer. The half-width $W_{1/2}$ of peak C_1, in contradiction to its potential, already depends on the type of electrode that is used. Peak C_1 is always significantly broader for the PIGE than for the paste electrode (Figures 7a and 7b, curve C_1). $W_{1/2}$ also depends on the structure of the PbO_2. Peak C_1 is about 70 mV broader for the β-PbO_2 than for α-PbO_2 (Figures 7c and 7d, curve C_1). These figures

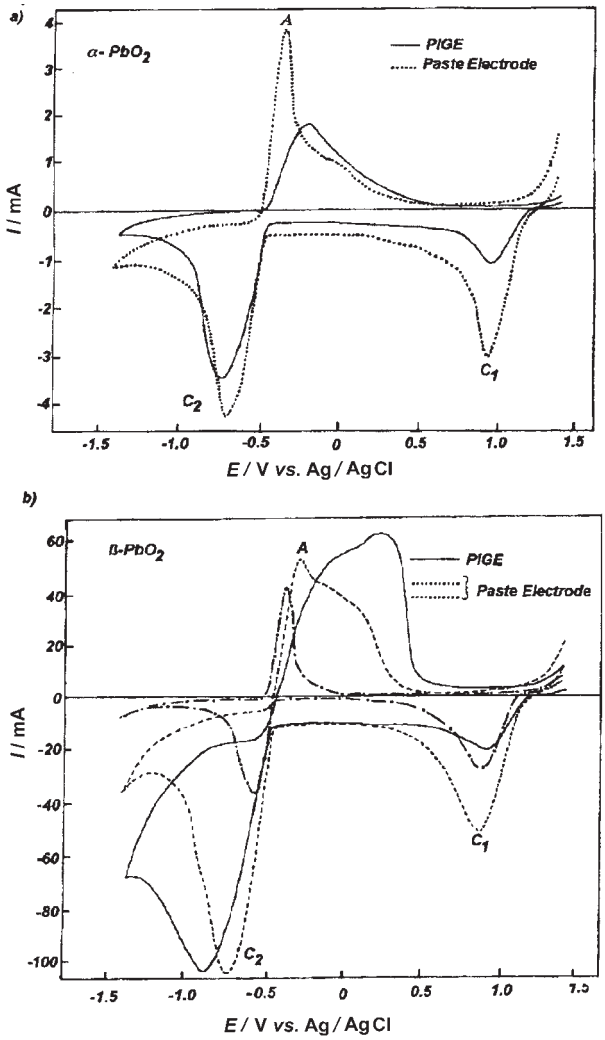

Figure 5. Typical cyclic voltammograms of (a) α-PbO_2 and (b) β-PbO_2 dispersed in graphite paste electrode (···, ---, –·–) and immobilized on the PIGE (—). Scan rate: 100 mV s^{-1}; electrolyte: 0.1 M HCl; concentrations of PbO_2 in the graphite paste: (···, ---) 2.0×10^{-4} mol g^{-1}; (–·–) 0.8×10^{-4} mol g^{-1}; starting potential: 1.4 V.

show that the $W_{1/2}$ of peak C_1 is always significantly smaller in case of the graphite paste electrode than in case of the PIGE, and it is smaller for α-PbO_2 than for β-PbO_2 at both electrodes. This means that the electrode process is more reversible at the paste electrode than at the PIGE, and the electrode process is more reversible for α-PbO_2 than for β-PbO_2.

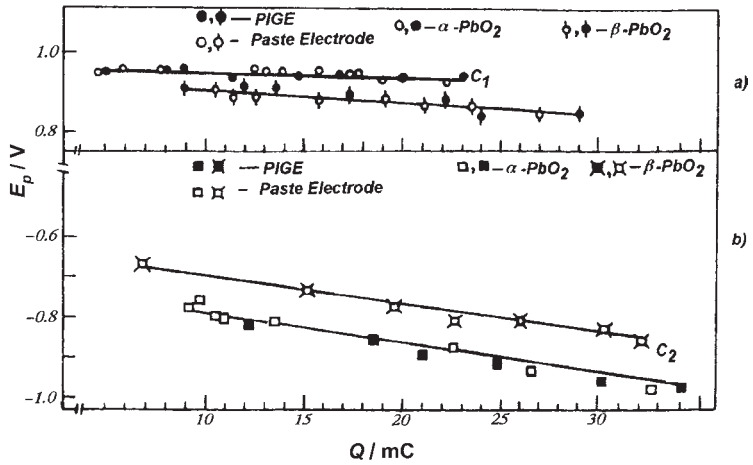

Figure 6. Plot of peak potentials of (a) C_1 and (b) C_2 *versus* the amount of charge consumed in the electrochemical conversions of α-PbO_2 (○, ●, □, ■) and β-PbO_2 (○, ●, □, ■) dispersed in the graphite paste electrode (○, ○, □, □) and immobilized on the PIGE surface (■, ■, ●, ●). Experimental conditions as in Figure 5.

The next step in the reduction of PbO_2 (peak C_2) depends in a complex way on the type of the electrode used and also on the structure of PbO_2. α-PbO_2 yields identical peak potentials for both electrodes (Figure 5a), which are determined by the amount of PbO_2 at the electrode surface (Figure 6b). The half-widths of the peaks (250 to 280 mV) depend only slightly on the amount of charge in case of the paste electrode. In case of the PIGE, the half-widths increase from 250 to 380 mV when the amount of charge increases from 10 to 34 mC (Figure 7b, curves C_2). For β-PbO_2, the line of E_p values of C_2 *versus* the amount of charge is situated about 85 mV more positive than the same line for α-PbO_2 (Figure 6b), and the shape of the peaks is very much determined by the amount of the substance at the electrode surface (Figure 5b). Peak C_2 is much sharper for β-PbO_2 than for α-PbO_2, if the concentration of the substance in the paste is equal or less than 8×10^{-5} mol g^{-1} (Figure 5b, curve –·–), but the values $W_{1/2}$ of β-PbO_2 will exceed those of α-PbO_2, if the concentration of the substance in the paste is higher than 2.5×10^{-4} mol g^{-1} (Figures 5b and 6d, curve C_2). This becomes visible only when the graphite paste electrode is used. Because of the complex form of peak C_2 when the PIGE is used (Figure 5b, curve –), the measurement of the consumed charge is not correct. Therefore, these data are not given in Figures 6 and 7. Figure 5b shows, however, that the second step of the reduction of β-PbO_2 at the PIGE proceeds with an overpotential of about 100 mV as compared to the reduction of this compound at the graphite paste electrode.

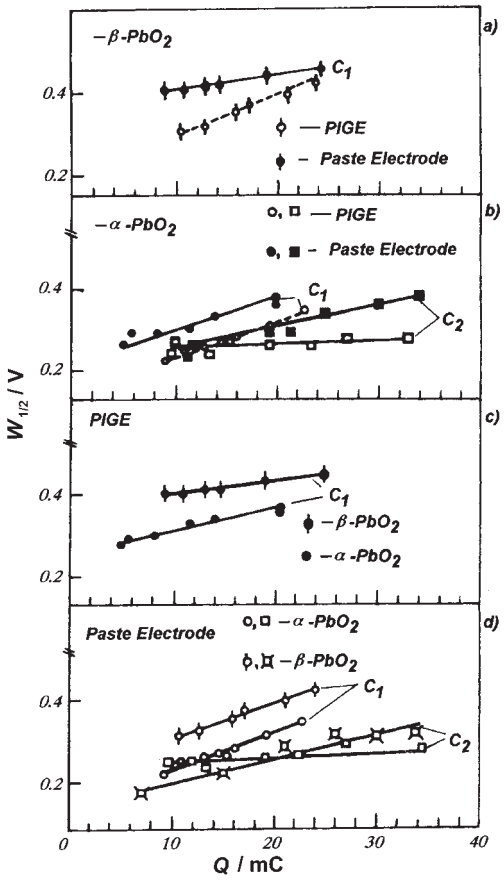

Figure 7. Plot of half-width of peaks (a) C_1 for β-PbO_2 at the PIGE (●) and at the paste electrode (○); (b) C_1 and C_2 for α-PbO_2 the at the PIGE (●, ■) and on the paste electrode (○, □); (c) C_1 for α-PbO_2 (●) and β-PbO_2 (●) at the PIGE; (d) C_1 and C_2 for α-PbO_2 (○, □) and β-PbO_2 (○, □) at the paste electrode *versus* the amount of consumed charge. Experimental conditions as in Figure 5.

Much more significant differences occur in the oxidation of cathodic reaction products (peak A). For α-PbO_2 (Figure 5a), in this oxidation, there is one particular signal, which is sharper in case of the paste electrode. Additionally, it is situated at more negative potentials in case of the paste electrode than of the PIGE. For β-PbO_2, peak A (Figure 5b) is usually divided into two badly separated peaks. This is especially typical of the PIGE. Signal A had a fully symmetric form when the amount of the β-PbO_2 in the graphite paste was reduced to amounts of less than 1×10^{-4} mol g^{-1} graphite powder (curve –·–, Figure 5b).

From scheme (10), it follows that the areas below peaks C_1, C_2 and A should be equal. In Table I, the areas below peaks C_1, C_2 and A are compared. The Table shows that the area below peak C_1 is 2.5 times smaller than the area below peak C_2 (for α-PbO_2). For the graphite paste electrode, the areas below peaks C_1 and C_2 are roughly equal to each other, *i.e.* for all concentrations of α-PbO_2 in the graphite paste. $Q(C_1)/Q(C_2)$ values will be always smaller than 1, if the solution is stirred during the experiment. This will also apply to β-PbO_2, if the concentration of the compound in the paste is smaller than 1×10^{-4} mol g^{-1}. The ratio $Q(C_2)/Q(A)$ will be always near to 1, if the ratio $Q(C_1)/Q(C_2)$ is equal or higher than 1.

All this indicates that the processes that we observe are more complicated than the simple reactions (5) to (9). Obviously, in case of the PIGE, at peak C_1, there is not the entire amount of PbO_2 consumed but only a certain part of it (reactions which are similar to (7) – (8) may proceed only partially). As $Q(C_1)/Q(C_2)$ will be always smaller than 1, if the solution is stirred, reactions as formulated in Eq. (5) will take place. Such reactions preferably occur with α-PbO_2. The presence of chloride ions in the electrolyte shifts the formal potential of such reactions to more negative potentials. Because of

TABLE I

The ratio between the charges consumed in the stepwise reduction of PbO_2 and the following oxidation of the cathodic reaction products ($n = 5$, $P = 0.95$)

PIGE			
α-PbO_2		β-PbO_2	
$Q(C_1)/Q(C_2)$	$Q(C_2)/Q(A)$	$Q(C_1)/Q(C_2)$	$Q(C_1)/Q(A)$
0.33 ± 0.12	1.20 ± 0.06	It is not correctly determined	

Graphite paste electrode			
Concentration $> 1 \times 10^{-4}$ mol g^{-1}			
α-PbO_2		β-PbO_2	
$Q(C_1)/Q(C_2)$	$Q(C_2)/Q(A)$	$Q(C_1)/Q(C_2)$	$Q(C_2)/Q(A)$
1.08 ± 0.09	0.99 ± 0.07	0.75 ± 0.05	1.20 ± 0.03
Concentration $< 1 \times 10^{-4}$ mol g^{-1}			
α-PbO_2		β-PbO_2	
$Q(C_1)/Q(C_2)$	$Q(C_2)/Q(A)$	$Q(C_1)/Q(C_2)$	$Q(C_2)/Q(A)$

the rough surface of the graphite paste electrode and its large adsorption capacity, the soluble products of the reaction cannot easily disappear from the electrode surface during the experiment, and one observes a well-developed response of the reduction of $Pb^{2+}_{(gr.)}$ to $Pb^{o}_{(gr.)}$ (peak C_2). In this case, $Q(C_1)/Q(C_2)$ almost equals 1. Peak A has characteristics, which are similar to the anodic stripping peak of lead in 0.1 M HCl.[10–12] For larger amounts of β-PbO_2 and in case of the PIGE, the processes of successive reduction are more complicated. Because of larger agglomerates of the substance on the electrode surface, the solution reaction (5) has not enough time to be completed, and the solid-state reactions (7) to (8) occur at the electrolyte/PbO_2/graphite interface. Most probably, the reaction of PbO_2 leads to the formation of layers of lower oxides, which are known to be poor conductors.[35] When PbO_2 is reduced at – 1.5 V *vs.* Ag/AgCl in contact with a neutral electrolyte and when, at a later time, the lead is oxidised during an anodic scan, one observes an almost ohmic line at negative potentials, and the entire oxidation peak exhibits a strong ohmic distortion (Figure 8). The formation of poorly conducting films of lower lead oxides will stop the further reduction. The reduction process can be formulated as follows:

$$PbO_2 + 2xH^+ + 2xe^- \rightarrow PbO_{2-x(\text{solid})} + xH_2O \text{ (peak } C_1) \qquad (11)$$

At peak C_2, the lower lead oxides, including PbO, are reduced to metallic lead. It is possible that the reduction also includes that of dissolved Pb^{2+} ions:

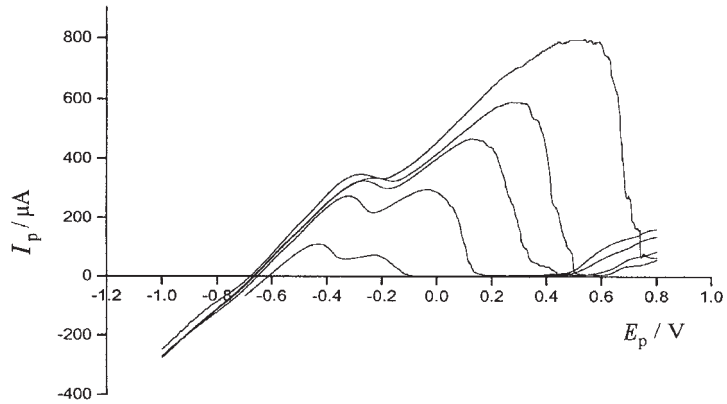

Figure 8. Typical anodic voltammograms of lead, which was obtained by the reduction of PbO_2 mechanically attached to a PIGE. Reduction potential: – 1.5 V; electrolyte: 0.1 M KNO_3.

$$Pb^{2+}_{(gr.)} + PbO_{2-x(solid)} + 2(2-x)H^+ + (2(2-x)+2)e^- \rightarrow Pb^{o}_{(gr.)} + Pb^{o}_{(solid)} + (2-x)H_2O \quad (12)$$

From this, it follows that the ratio of charges $Q(C_1)/Q(C_2)$ is smaller than 1 and that the ratio $Q(C_2)/Q(A)$ is always higher than 1. Just this can be observed in experiments. The fact that the half-width of signal C_2 is larger and more strongly depending on the amount of consumed charge in case of the PIGE ($dW_{1/2}/dQ$ = 6 mV/mC, Figure 7b, curve –■–) than in case of the graphite paste electrode ($dW_{1/2}/dQ$ = 1 mV/mC, Figure 7b, curve –□–) can be easily explained by the fact that a nonconducting film will affect the measurement more strongly when a PIGE electrode is used than in case of a graphite paste electrode where insulating particles are very effectively embedded in the graphite. This also influences the shape of the anodic signal A. A certain amount of lead is present at the electrode surface in close contact with the graphite. This lead is oxidized at the sharp and more negative part of A. This part of the signal is identical with the usual anodic stripping signal of lead after plating Pb from solutions. The broad shoulder of A at more positive potentials is most probably due to the oxidation of lead which was formed in a solid-state reduction of PbO_2 and which does not so well adhere to the graphite particles. Obviously, the signal, which is obtained when lead is plated from a solution, is observed in case of α-PbO_2 (Figure 5a, curve ···) and also in case of small amounts of β-PbO_2 (Figure 5b, curve –·–) in the graphite paste electrode. As is the case with PbO, no response of a further oxidation ($Pb^{2+} \rightarrow Pb^{4+}$) has been ever observed in a hydrochloric acid electrolyte.

$BaPbO_3$

Figure 9 shows typical cyclic voltammograms of the electrochemical conversion of $BaPbO_3$ at the PIGE (a) and at the graphite paste electrode (b) in 0.1 M HCl. The voltammograms were recorded in the potential range from 1.2 to –1.5 V at a scan rate of 100 mV s^{-1}. It is generally assumed that the oxidation state of lead is 4+ in the $BaPbO_3$ phase. In this connection, we expected that the voltammetry of this phase will resemble the voltammetry of PbO_2. Unlike in case of PbO_2, where the reduction of the studied substance occurs in two subsequent steps (peak C_1 and C_2, Figure 5), we observed four peaks (C_0, C_1, C_2, C_3) in this case. The anodic signals A_1 and A_2 are practically identical with those of PbO (Figure 1). The first two signals (C_0 and C_1) vanish during the following cycles, both in case of the PIGE (Figure 9a) and the graphite paste electrode (Figure 9b). Peak C_3 also vanishes when the PIGE is used and significantly decreases in case of the graphite paste

electrode. Signal A_1 only occurs in the second cycle but decreases in the third cycle, peak A_2 also decreases, and peak A_3 is never observed when $BaPbO_3$ is studied using the PIGE. Under the same experimental conditions, but using the graphite paste electrode, peak A_1 does not change,

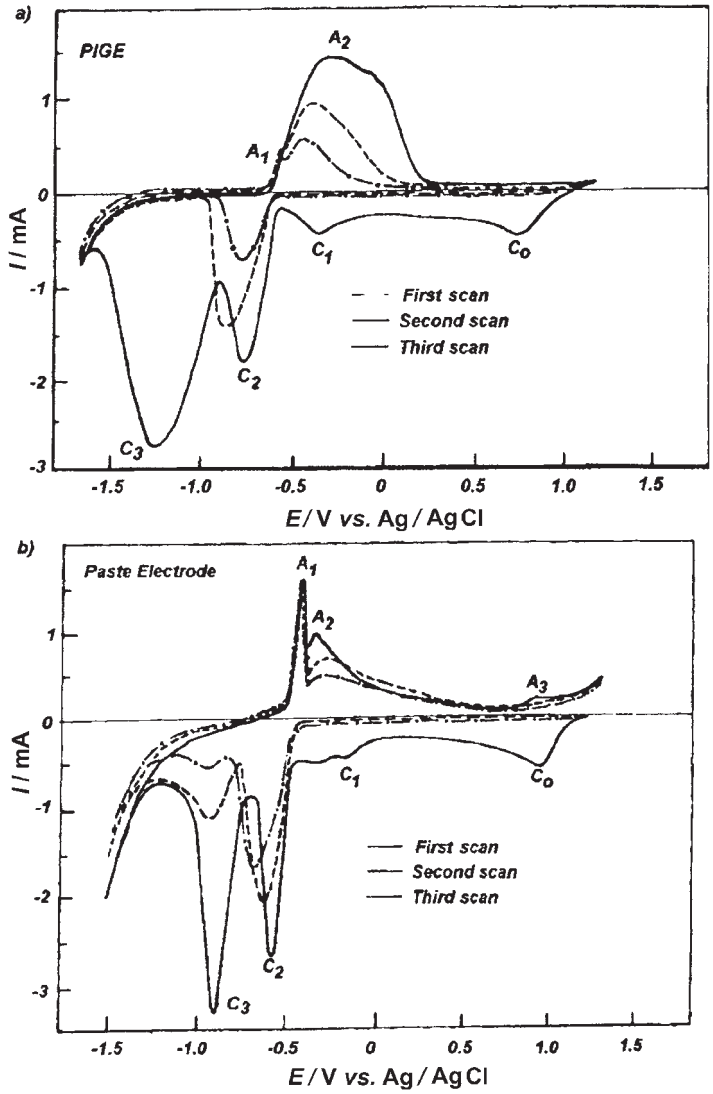

Figure 9. Typical cyclic voltammograms of $BaPbO_3$ (a) immobilized at the PIGE surface and (b) dispersed in a graphite paste electrode. Scan rate: 100 mV s^{-1}; electrolyte: 0.1 M HCl; starting potential: 1.2 V.

whereas peak A_2 decreases and becomes broader. Peak A_3 occurs in the first cycle only. All observed signals are better developed in case of the graphite paste electrode than in case of the PIGE. Figure 10 shows cyclic voltammo-

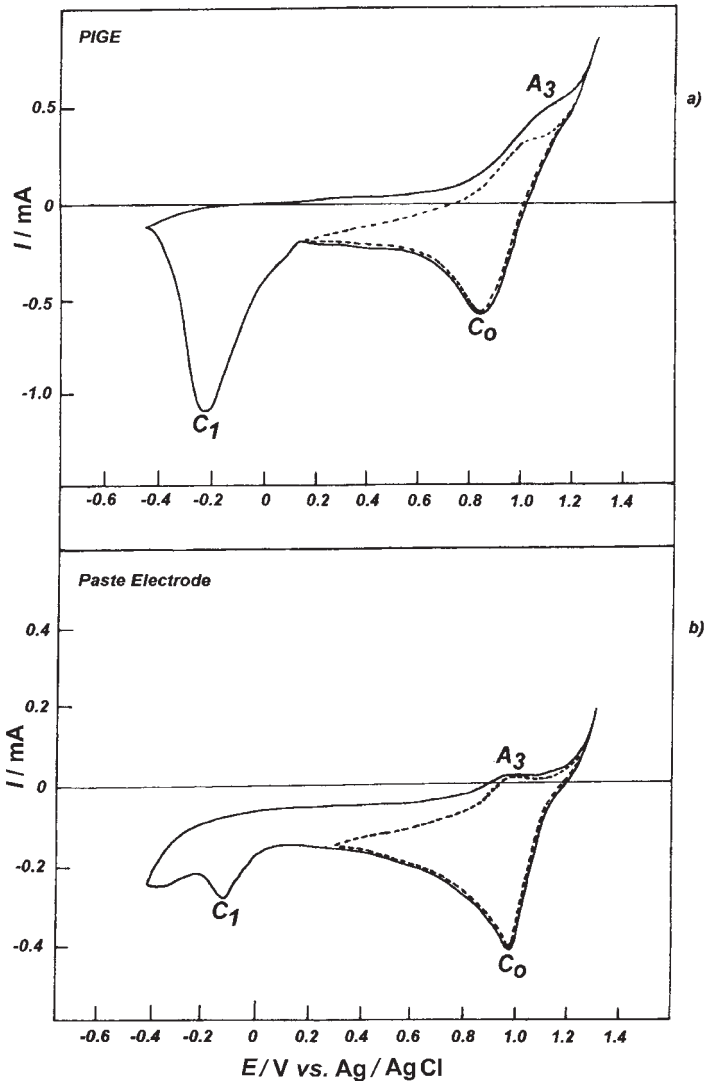

Figure 10. Typical cyclic voltammograms of $BaPbO_3$ (a) immobilized at the PIGE surface and (b) dispersed in a graphite paste electrode recorded in range potential from 1.2 to – 0.4 V (—) and from 1.2 to 0.2 V (---). Scan rate: 100 mV s^{-1}; electrolyte: 0.1 M HCl; starting potential: 1.2 V.

grams of $BaPbO_3$ recorded in a limited potential range from 1.2 V to –0.4 V and from 1.2 V to 0.2 V to exclude the interference of products of peaks C_2 and C_3 in the elucidation of peaks C_0 and C_1. Peak C_1 was not present in the voltammetry of PbO_2. As can be seen from Figure 10, there is no separate anodic signal indicative of an oxidation of cathodic reaction products of C_1. There is one anodic peak A_3 that corresponds to the cathodic peaks C_0. Peak A_3 never occurs when the solution is stirred. Therefore, it is assumed that peak C_0 corresponds to a reduction of Pb^{4+} in the electrode layer after a preliminary chemical reaction of the type:

$$BaPbO_3 + 6H^+ \rightarrow Ba^{2+} + Pb^{4+}_{(gr.)} + 3H_2O \quad (13)$$

$$Pb^{4+}_{(gr.)} + 2e^- \rightarrow Pb^{2+}_{(gr.)} \ (\text{peak } C_0) \quad (14)$$

Then peak C_1 may correspond to the solid-phase reaction:

$$BaPbO_3 + 2H^+ + 2e^- \rightarrow BaPbO_2 + H_2O \quad (15)$$

The limited rate of transport of H^+-ions in the solid phase may cause a retardation of the following electrochemical oxidation of $BaPbO_2$. In addition, in contrast to $BaPbO_3$, which has metallic conductivity,[36, 37] $BaPbO_2$ is dielectric. The formation of a poorly conducting film may stop the further reduction and subsequent oxidation. Therefore, the Pb^{2+} ions from reaction (14) may be crucial only for peak A_3.

As can be seen from Figure 9, only an insignificant part of the entire $BaPbO_3$ is reduced in the course of reactions (13–15). Probably, these reactions are only confined to a surface layer. The electrochemical conversion of the bulk phase of $BaPbO_3$ occurs at peaks C_2 and C_3. Metallic lead is the product of these electrochemical reactions. Shape and position of A_1 and A_2 are indicative of this. The ratio of the areas below peaks C_2 and C_3 to the areas below peaks A_1 and A_2, *i.e.* $Q(C_1 + C_2) / Q(A_1 + A_2)$, is equal to 2, within the limits of experimental error ± 0.15 for $n = 5$ and $P = 0.95$. This indicates that four electrons are involved in the reduction of $BaPbO_3$. Studying the features of the phase formation and properties of $BaPbO_3$, the authors[36] have shown that the samples are microinhomogeneous. They change both their structure and morphology in the thermotreatment process. The lead ions are present in two oxidation states, Pb^{4+} and Pb^{2+}. We think that all these features influence the electrochemistry of $BaPbO_3$. Only thin surface layers (≈ 50 μm)[36] take part in the reduction at peaks C_0 and C_1 (13–15). The bulk of $BaPbO_3$ is stepwise reduced at peaks C_2 and C_3:

Peak C_2,

$$BaPb^{IV}_{1-x}Pb^{II}_{x}\ {}_{x}O_3 + 4xH^+ + 4xe^- \rightarrow BaPb^{IV}_{1-2x}Pb^{II}_{2x}O_{3-2x} + 2xH_2O \quad (16)$$

and peak C_3,

$$BaPb^{IV}_{1-2x}Pb^{II}_{2x}O_{3-2x} + 4(1+x)H^+ + 4(1+x)e^- \rightarrow Ba(OH)_2 + Pb^0 + (1+2x)H_2O \quad (17)$$

where is a hole with a 2+ charge.

The anodic signals A_1 and A_2 correspond to the cathodic peaks C_2 and C_3. The solid phase $BaPbO_3$ will be gradually consumed during the subsequent cycles, if the graphite paste electrode is used (Figure 9b), but signal C_3 will vanish already after the first cycle if the PIGE is used (Figure 9a). The cyclic voltammograms are very similar to those of PbO (Figure 1) because in this case signal C_2 is due to the reduction of PbO as a product of the electrode reaction which is responsible for the arising of peaks A_1 and A_2. Because of the complex shape of the voltammograms, we could not study the dependence of $E_p(C_1)$ on Q.

Electrochemical Behaviour of Lead Oxides in Contact with an Alkaline Electrolyte

There is information available about the voltammetric behaviour of PbO,[11] PbO and PbO_2,[23] α-and β-PbO_2 [29] in 0.1 M NaOH [11,23] and 4.7 M NaOH [21,22] aqueous solutions. 1 M aqueous NaOH solution was used as a supporting electrolyte in our work. We think that such a concentration is more acceptable for the experiments since it is not as high as in Refs. 29 and 30 but eliminates the possibility of hydrolysis in the electrode layer as it is possible in Ref. 11 and 23.

PbO

Figure 11 shows typical cyclic voltammograms of red PbO at the PIGE and at the graphite paste electrode in the potential range 1.0 V and –1.5 V (starting at –0.4 V). With both electrodes the reduction of PbO proceeds practically at the same peak (C_1) potential and shifts to more negative values with increasing amounts of PbO at the surface of the electrode (Figure 12a). In case of the PIGE, the ascending part of the reduction signal is usually

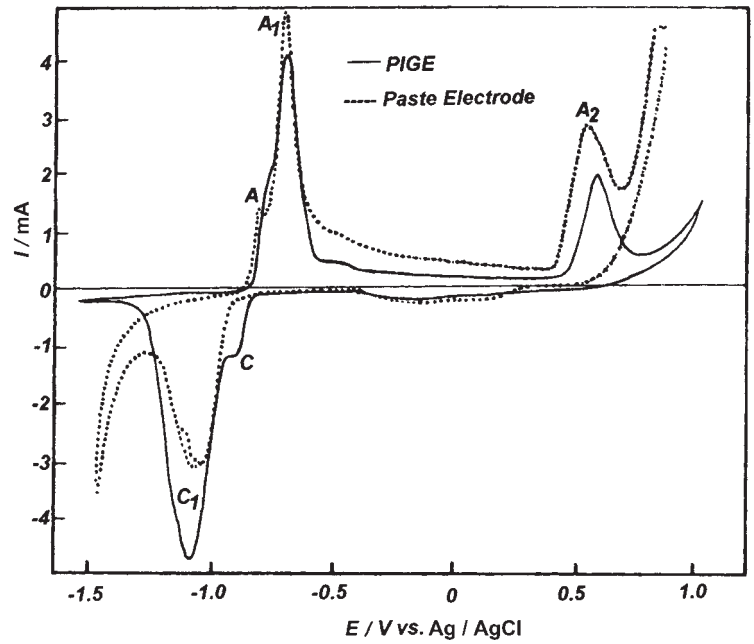

Figure 11. Typical cyclic voltammograms of PbO dispersed in the graphite paste electrode (···) and immobilized on the PIGE surface (—). Scan rate: 100 mV s^{-1}; electrolyte: 1 M NaOH; starting potential: – 0.4 V.

complicated by the occurrence of the shoulder C. This is very similar to what has been described[23] for the graphite paste electrode with the 0.1 M NaOH solution as binder. The authors[23] suppose that signal C corresponds to the reduction of a small amount of $HPbO_2^-$ formed by the chemically dissolution of PbO according to

$$PbO + OH^- \rightarrow HPbO_2^- \quad (18)$$

$$HPbO_2^- + H_2O + 2e^- \rightarrow Pb^o + 3OH^- \quad (19)$$

whereas peak C_1 is most probably due to the electrochemically induced[34] solid-state reduction of PbO:

$$PbO + H_2O + 2e^- \rightarrow Pb^o + 2OH^- \quad (20)$$

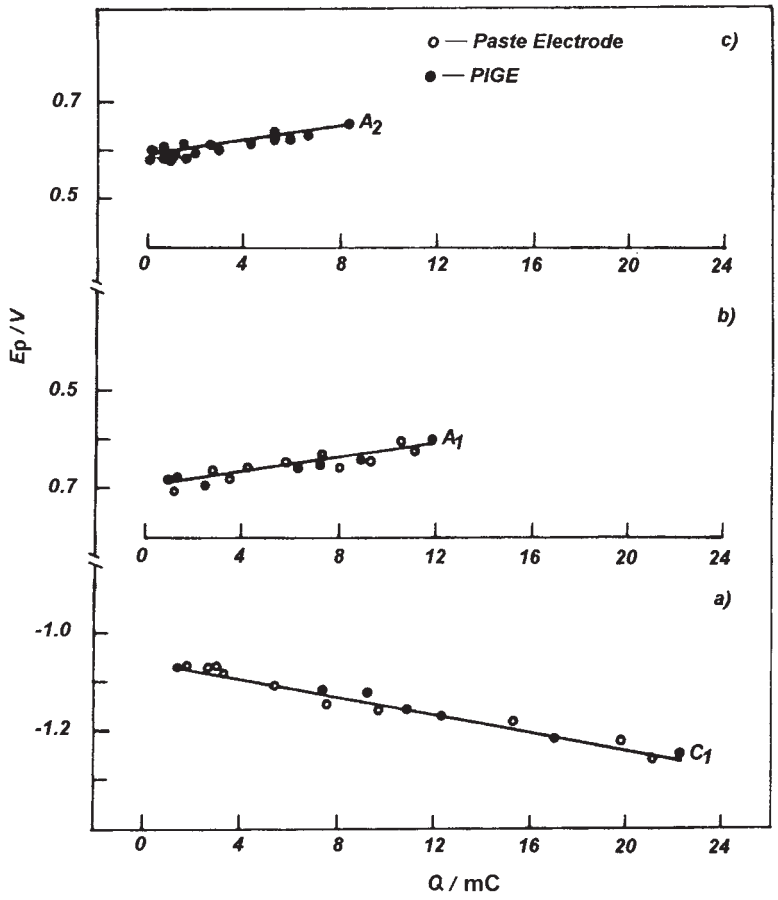

Figure 12. Plot of peak potentials of (a) C1, (b) A1 and (c) A2 for the electrochemical conversions of PbO dispersed in the graphite paste electrode (–○–) and immobilized at the PIGE surface (–●–). Experimental conditions as in Figure 11.

In case of the graphite paste electrode with the organic binder, the reaction (18) is inhibited and practically all PbO is reduced *via* reaction (20). The voltammograms following the first cycle (Figure 13) indicate that the share of the reactions (18) and (19) increases with time. The increase in the peak currents of all peaks is possibly caused by the introduction of increasing amounts of the paste into the electrode reaction because of an increasing roughening[21] of the paste surface which itself is caused by the oxygen evolution occurring at potentials more positive than 0.9 V. This can also be derived from the increasing background current at positive potentials (see Figures 11 and 13a). The opposite effect is observed in case of the PIGE, *i.e.*

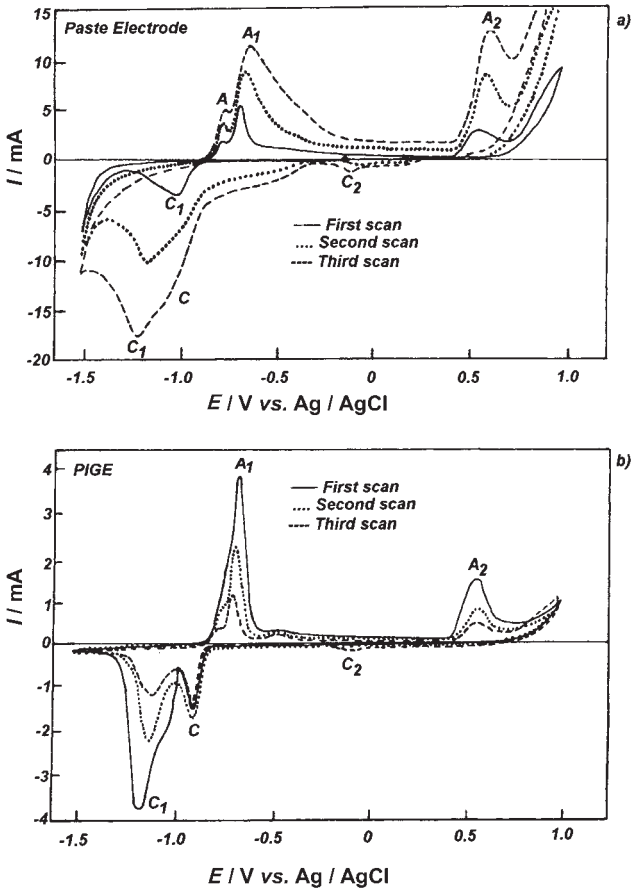

Figure 13. Typical first three voltammograms of PbO dispersed in the graphite paste electrode (a) and immobilized at the PIGE surface (b). Scan rate: 50 mV s^{-1}; electrolyte: 1 M NaOH; starting potential: –0.1 V.

all peaks decrease after cycling (Figure 13b). Sometimes the descending part of peak C_1 is also complicated when the paste electrode is used. Possibly, the partial overlapping of signal C and peak C_1 causes the half-width of the peak to increase more, with increasing amounts of PbO in case of the PIGE as compared to the graphite paste electrode (Figure 14a). In contrast to the hydrochloric acid solution, we observe two steps of electrochemical oxidation of metallic lead ($Pb^o \rightarrow Pb^{2+} \rightarrow Pb^{4+}$, peaks A_1 and A_2) when 1 M NaOH is used as a supporting electrolyte. The potential and half-width of these peaks do not depend on the electrode used (Figures 12b, 12c and 14b). Apparently, the anodic peak A_1 is due to the following reaction:

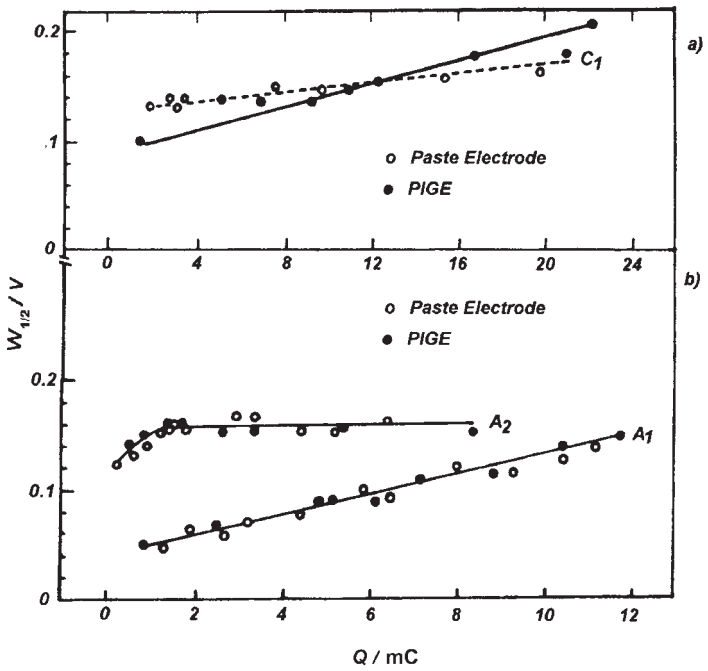

Figure 14. Plot of the half-width *versus* the amount of consumed charge of peaks (a) C_1 and (b) A_1, A_2 for the electrochemical conversions of PbO dispersed in the graphite paste electrode (–○–) and immobilized at the PIGE surface (–●–). Electrolyte: 1 M NaOH. Experimental conditions as in Figure 11.

$$Pb^{o} + 3OH^{-} - 2e^{-} \rightarrow HPbO_2^{-} + H_2O \text{ (peak } A_1) \quad (21)$$

The resulting ions $HPbO_2^{-}$ are further oxidized according to:

$$HPbO_2^{-} + 3OH^{-} - 2e^{-} \rightarrow PbO_3^{2-} + 2H_2O \text{ (peak } A_2) \quad (22)$$

The half-width of this peak depends on the consumed charge only for small amounts of reacting substance (Figure 14b, curve A_2). We suggest that the anodic response A corresponds to shoulder C. Signal A is less developed for the PIGE. It is possible that the signal splitting in case of the graphite paste electrode is caused by the higher dispersity of the electrode surface. The cathodic peak C_2 occurring in the third cycle corresponds to the reduction of PbO_3^{2-} anodically formed at peak A_2. When the solution is stirred, signal C_2 is never observed. This means that reaction (22) produces

soluble products only. Peak C_2 occurs already in the second cycle when a graphite paste electrode is used with an electrolytic binder.[23] In principle, our results are identical with the results reported in Reference 23. A small shift of the reduction potentials to more negative values and a shift of the oxidation potentials to more positive values in our experiments is due to an increased concentration of the electrolyte. But $W_{1/2}$ (< 200 mV) is always smaller in our case than it has been observed (> 270 mV) in Ref. 23. This means that the electrochemical conversions of PbO are more reversible at the PIGE and at the graphite paste electrode with the oil as a binder than those at the carbon paste electrode having an electrolytic binder.

α-PbO_2 and β-PbO_2

Centeno *et al.*[23] studied the voltammetry of lead dioxide in graphite paste electrodes with an electrolyte binder (0.1 M NaOH) and discussed the mechanism of some reactions. Unfortunately, there is no information about the modification of PbO_2, which has been studied by them. Chartier and Poisson[31] have studied the cathodic reaction of α- and β-PbO_2 electrodes in alkaline electrolytes and found that the mechanism of reduction differs for the two polymorphs. For β-PbO_2, it has been suggested that the electrode reaction mechanism consists of two processes: (a) a dissolution reaction:

$$\alpha\text{-}PbO_2 + H_2O + 2e^- \rightarrow HPbO_2^- + OH^- \tag{23}$$

and (b) a solid-phase reaction:

$$\beta\text{-}PbO_2 + H_2O + 2e^- \rightarrow PbO + 2OH^- \tag{24}$$

For α-PbO_2, they suggested that the reduction process occurs exclusively in the solid phase but they were unable to give an exact mechanism. Carr and Hampson[29,30] concluded that the adsorption of electrode products is involved in the electrode reaction of α-PbO_2. They proposed the following sequence of reactions:

$$\alpha\text{-}PbO_2 + H_2O + 2e^- \rightarrow PbO_{ads} + 2OH^- \tag{25}$$

$$PbO_{ads} \rightarrow PbO_{aq}$$

$$PbO_{aq} + OH^- + H_2O \rightarrow Pb(OH)_3^-$$

where PbO_{ads} and PbO_{aq} represent PbO adsorbed at the interphase and dissolved in solution, respectively. A further reduction to Pb^o has not been discussed by the authors.[29]

The cyclic voltammograms of both modifications of PbO_2 were recorded from 1.0 V to –1.5 V at a scan rate of 100 mV s^{-1} (see Figure 15). As in the case of hydrochloric acid, two cathodic peaks (C_1 and C_2) occur but the separation of peaks C_1 and C_2 is better. In principle, this effect has been also observed by Centeno *et al.*[23] but these authors have not paid attention to the difference in peak sizes and describe these peaks with the following reactions:

$$PbO_2 + 2OH^- \rightarrow PbO_3^{2-} + H_2O$$

$$PbO_3^{2-} + 2H_2O + 2e^- \rightarrow HPbO_2^- + 3OH^- \text{ (peak } C_1) \qquad (26)$$

and the subsequent reduction process:

$$HPbO_2^- + H_2O + 2e^- \rightarrow Pb^o_{(s)} + 3OH^- \text{ (peak } C_2) \qquad (27)$$

There are no differences in the peak potentials of peak C_1 of α- and β-PbO_2 for both the PIGE and the graphite paste electrode (Figure 16a) when the amount of PbO_2 is very small (< 2 mC). These peak potentials are less positive than those for the graphite paste electrode with an electrolytic binder (0.1 M NaOH),[23] but more negative than those for the electrode with lead dioxide electrodeposited onto platinum.[29,30] The difference in the peak potentials of C_1 occurs for α- and β-PbO_2 when the amount of reacting PbO_2 at the electrode surface ranges from 2.5 to 10 mC. In this case, the potential of peak C_1 of α-PbO_2 shifts from – 0.12 to –0.15 V while that of β-PbO_2 shifts from – 0.12 to –0.22 V (Figure 16a) with a confidence range of ±0.02 V (n = 5, P = 0.95). At the lead dioxide electrode, the difference between E_p(α-PbO_2) and E_p(β-PbO_2) reaches 0.12 V in 4.7 M NaOH.[29] The half-width of peak C_1 depends on the electrode used (Figure 17a). $W_{1/2}$ is always smaller for the PIGE than for the graphite paste electrode. There are no differences in the half-width of α- and β-PbO_2 peaks when the PIGE is used (Figure 17a). When the graphite paste electrode is used under the same conditions, the half-width of peak C_1 is much bigger, especially for higher amounts of α-PbO_2 (Figure 17a). In case of β-PbO_2, the half-width of peak C_1 slightly depends on the amount of reacting PbO_2, and independently of Q, the difference between the half-widths of the PIGE and the graphite paste electrode remains practically constant (about 40 mV). Besides, when the solution is

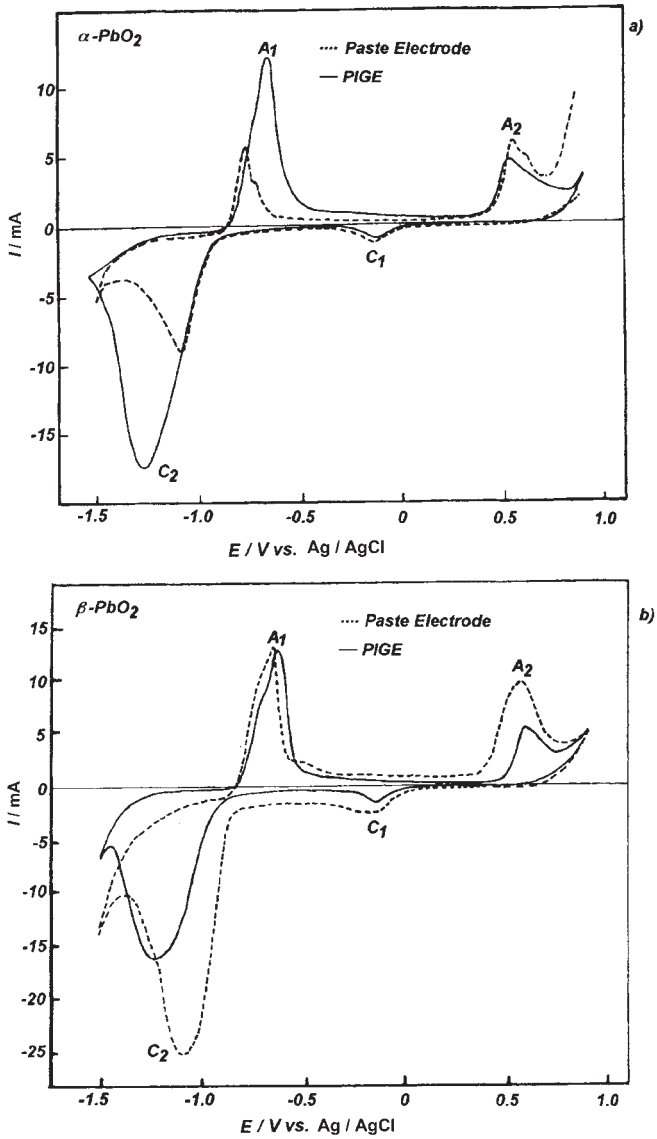

Figure 15. Typical cyclic voltammograms of (a) α-PbO_2 and (b) β-PbO_2 dispersed in the graphite paste electrode (---) and immobilized at the PIGE surface (—). Scan rate: 100 mV s^{-1}; electrolyte: 1 M NaOH; starting potential: 1.0 V.

stirred, signal C_1 decreases to a constant value for both electrodes. Under the same conditions, peak C_1 remains practically constant for α-PbO_2. It seems that in our case the first step of the electrochemical reduction mecha-

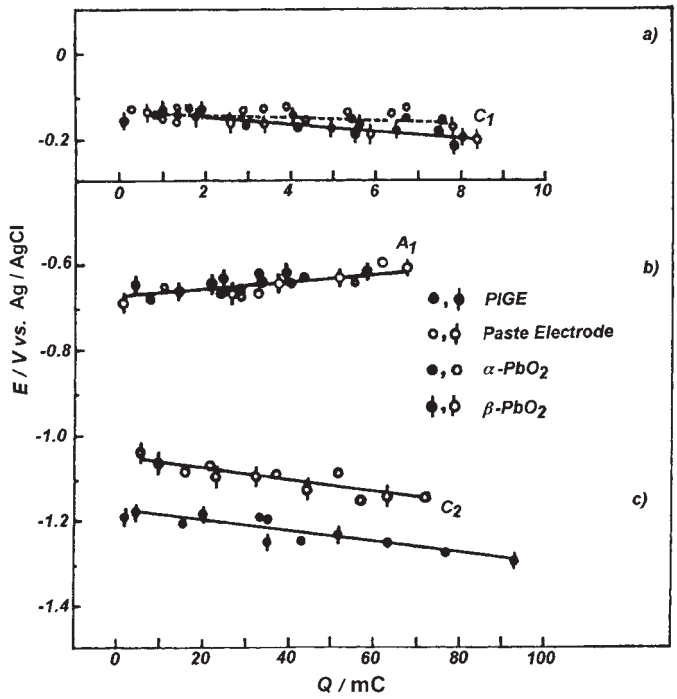

Figure 16. Plot of peak potentials *versus* the amount of consumed charge of (a) C_1, (b) A_1 and (c) C_2 for the electrochemical conversions of α-PbO_2 (–○–, –●–) and β-PbO_2 (–○–, –●–) dispersed in the graphite paste electrode (–○–,–○–) and immobilized at the PIGE surface (–●–, –●–). Experimental conditions as in Figure 15.

nism of α- and β-PbO_2 is not different from the mechanism suggested for the reduction of lead dioxides deposited onto platinum.[21] The reduction process of α-PbO_2 occurs exclusively in the solid phase according to scheme (25). For β-PbO_2, the electrode reaction mechanism consists of (a) a dissolution reaction (23) or (26) and (b) a solid-phase reaction (24).

The second step of PbO_2 reduction (peak C_2, Figure 15) occurs at potentials below –1.05 V for the graphite paste electrode, and below –1.17 V for the PIGE (Figure 16c). This peak is narrower for the paste electrode than for the PIGE (Figure 17b). There are no differences between the peak potentials and half-widths of α- and β-PbO_2. The slope of a plot of E_p *vs.* Q is the same for both electrodes (11 ± 1 mV/mC), which is also true of peak C_1 in case of PbO reduction (Figure 12a). In contradiction to PbO, where the ratio $Q(C_1)/Q(A)$ was about 1, for PbO_2 the ratio $Q(C_2)/Q(A_1)$ is 1.9 ± 0.2. This indicates that the main part of PbO_2 is reduced in a $4e^-$ step at peak C_2. The

potential and half-width of the anodic peak A_1 neither depend on the kind of electrode nor on the structural modification of PbO_2 (Figures 16b and 17c). Though, for the PIGE, there is a larger difference between the charges of peak A_1 and A_2, these two peaks have almost equal charges in case of the graphite paste electrode (Figure 15). The potential of peak A_2, which corre-

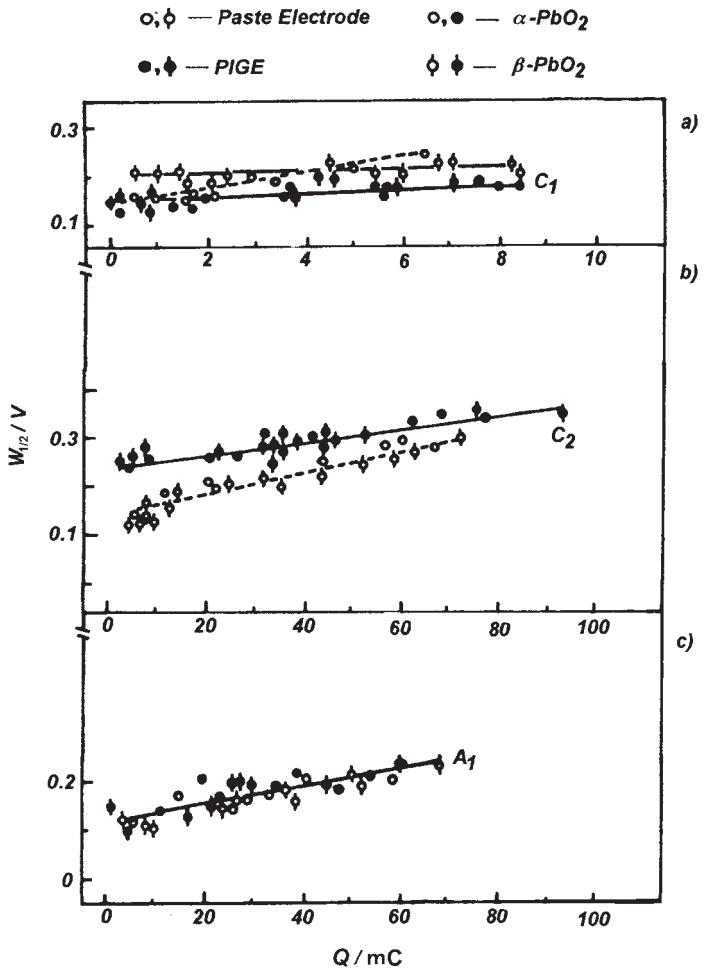

Figure 17. Plot of half-width of peaks *versus* the amount of consumed charge of (a) C_1, (b) C_2 and (c) A_1 for the electrochemical conversions of α-PbO_2 (–○–, –●–) and β-PbO_2 (–○–, –●–) dispersed in the graphite paste electrode (–○–, –○–) and immobilized at the PIGE surface (–●–, –●–) in contact with an 1 M NaOH electrolyte. Experimental conditions as in Figure 15.

sponds to the further oxidation of Pb^{2+}, is almost independent of the experimental conditions. It is necessary to note that at low scan rates (5–10 mV s^{-1}) and with a low concentration of PbO_2 in the paste (1×10^{-4} mol g^{-1}), a linear relationship between $I_p(C_2)$ and $\sqrt{\nu}$ passing through the origin is observed for both lead dioxides. This indicates that diffusion is limiting the currents. The authors[29] observed the same plot of I_p *vs.* $\sqrt{\nu}$ and explained this by the diffusion of OH^- ions in the solution toward the electrode surface. They have calculated the diffusion coefficient of OH^- ions for the reduction of α-PbO_2 in alkaline solution. The obtained value of 10^{-7} cm^2 s^{-1} is too small to be the true diffusion coefficient of the OH^- ions in aqueous solution. These data can be interpreted by a possible diffusion of OH^- ions through a PbO layer or, more probably, of H^+ only, at the electrode surface at peak C_1. At higher scan rates and/or higher concentrations of PbO_2, a linear relationship between I_p and $\sqrt{\nu}$ is also observed but it does not pass through the origin. In this case the current limitation can be due to the diffusion of ions in a film of PbO formed at the electrode surface at the peak C_1. A tentative explanation of the observed effects can be formulated as follows:

$$\{2PbO_2\}PbO + 3OH^- \rightarrow HPbO_2^- + \{PbO_3^{2-}\} + H_2O \quad (28)$$

$$\{PbO_3^{2-}\} + 3H_2O + 4e^- \rightarrow Pb^o + 6OH^- \quad (29)$$

$$HPbO_2^- + H_2O + 2e^- \rightarrow Pb^o + 3OH^- \quad (30)$$

where $\{PbO_2\}PbO$ denotes the bulk phase $\{PbO_2\}$ covered by a surface layer of PbO which has been formed at C_1. Lamache and Bauer[15] have suggested that an electrochemically induced dissolution of a solid is well possible in the case of carbon paste electrodes and approached these reactions theoretically. From a thermodynamic point of view, reaction (29) may occur (Ref. 24, p. 232) at potentials more negative than the reaction of the solid-state reduction of PbO under the same conditions. May be that this is the reason why peak C_2 of PbO_2 is more negative than peak C_1 of PbO. For such reactions as (28–30), a direct interaction with ions of the electrolyte is necessary, and the amount of these ions in the electrode surface layer will be increased when the true surface of the electrode is roughened. Therefore, the peak potential of C_2 is more positive in case of the graphite paste electrode than in case of the PIGE. Because of the multistep nature of the overall reaction, the half-width of peak C_2 (Figure 17b) is considerably bigger for PbO_2 than for PbO (Figure 14b) although the number of electrons involved in the reduction is 4 for PbO_2 and 2 for PbO. It should be noted that the $W_{1/2}$ of C_2

(≤ 350 mV for the PIGE and ≤ 250 mV for the graphite paste electrode) and the $W_{1/2}$ of the same peak in Ref. 19 (350 mV) are comparable. Peaks A_1 and A_2 cannot be distinguished from those of PbO in alkaline electrolytes.

$BaPbO_3$

Cyclic voltammograms of barium metaplumbate (Figure 18) show that the reduction of this phase also occurs at two peaks, C_1 and C_2. But in this case $E_p(C_1)$ is shifted to more negative and $E_p(C_2)$ to more positive potentials than for PbO_2. The potentials of the anodic peaks A_1 and A_2 (≈ 0.6 V) are fully identical with the peaks of PbO and PbO_2. After the anodic signal A_2, peak A_3 (0.8 V) is always observed when a graphite paste electrode is

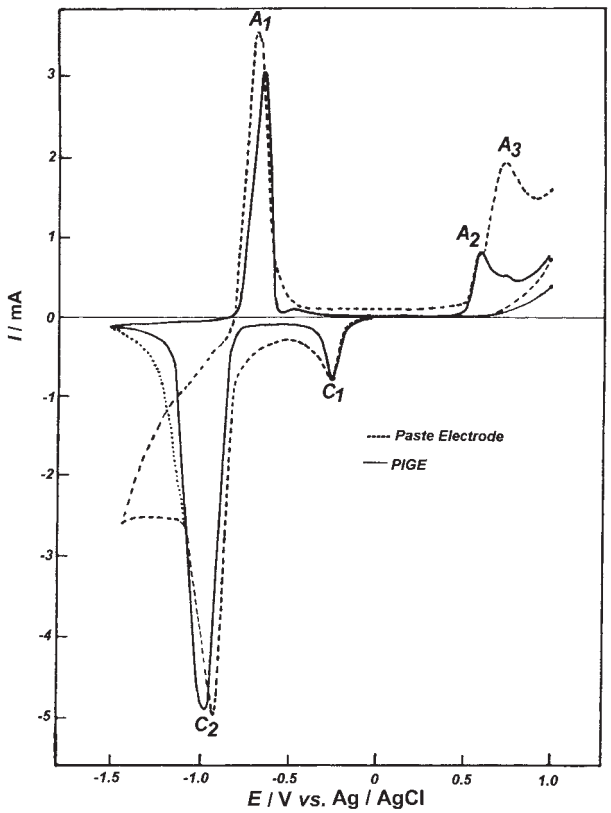

Figure 18. Typical cyclic voltammograms of $BaPbO_3$ dispersed in the graphite paste electrode (---) and immobilized at the PIGE surface (–). Scan rate: 100 mV s^{-1}; electrolyte: 1 M NaOH; starting potential: 1.0 V.

used. Peak A_3 will be only present, if the voltammograms are recorded in the potential range from 1 V to –0.4 V, *i.e.* when peaks C_2 and A_1 are not recorded (Figure 19). Under the same experimental conditions, signal A_3 will not occur, if a PIGE is used. Obviously, peak C_1 corresponds to the reduction process

$$BaPbO_3 + 2H_2O + 2e^- \rightarrow Ba(OH)_2 + HPbO_2^- + OH^- \quad (31)$$

It is possible that the very rough surface of the graphite paste electrode may serve as a trap for the $HPbO_2^-$ ions, and we observe the oxidation peak of this ion as signal A_3. It seems that a well-polished surface of the PIGE is not well suited for the accumulation of $HPbO_2^-$ ions on the electrode surface. It is possible that these ions diffuse away from the electrode layer and do not take part in a subsequent oxidation. The peak potential of C_1 does not depend on the kind of electrode used. A linear relationship between E_p and Q is observed with a slope of 2.5 mV/mC for both the PIGE and the graphite paste electrode (Figure 20a). Within the limits of experimental error (± 0.3), this is the same slope as it has been observed in the case of α- and β-PbO_2 on the graphite paste electrode (Figure 17a). Unlike PbO_2, the

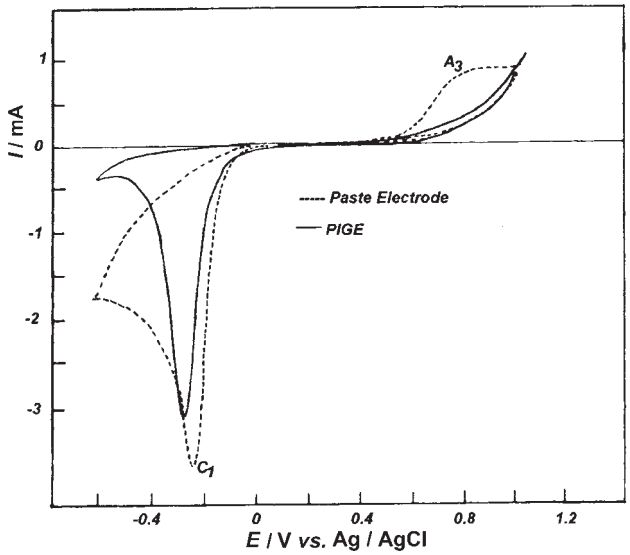

Figure 19. Typical cyclic voltammograms of $BaPbO_3$ dispersed in the graphite paste electrode (---) and immobilized at the PIGE surface (—). Scan rate: 50 mV s^{-1}; electrolyte: 1 M NaOH; starting potential: 1.0 V.

barium metaplumbate yields a plot of E_p *vs.* Q, which is situated at potentials which are about 120 mV more negative. The peak will be practically symmetrical and narrower, if a PIGE is used, especially for $Q > 10$ mC (Figure 21a). The following peak C_2 is also symmetrical and narrower for $BaPbO_3$ than for PbO_2 at the PIGE. If the graphite paste electrode is used, peak C_2 will be narrower for $BaPbO_3$ than for PbO_2, but the descending part of peak C_2 is partly obscured by the discharge of the supporting electrolyte. Therefore, an exact calculation of the area below the peak is not possible. For this reason, we determined the charge, which is consumed in the electrode reaction by extrapolation of the descending part of peak C_2 to the background current (see the dotted line for peak C_2 in Figure 18). The plot of $E_p(C_2)$ *vs.* Q has the same slope (15 ± 1 mV/mC) for both electrodes. This slope is only 4 mV/mC larger than the slope of the same plots for PbO (Figure 12a) and PbO_2 (Figure 16c). Unlike for PbO_2 and PbO, in the present case, the cathodic peak, which is responsible for peak A_1 occurs at more

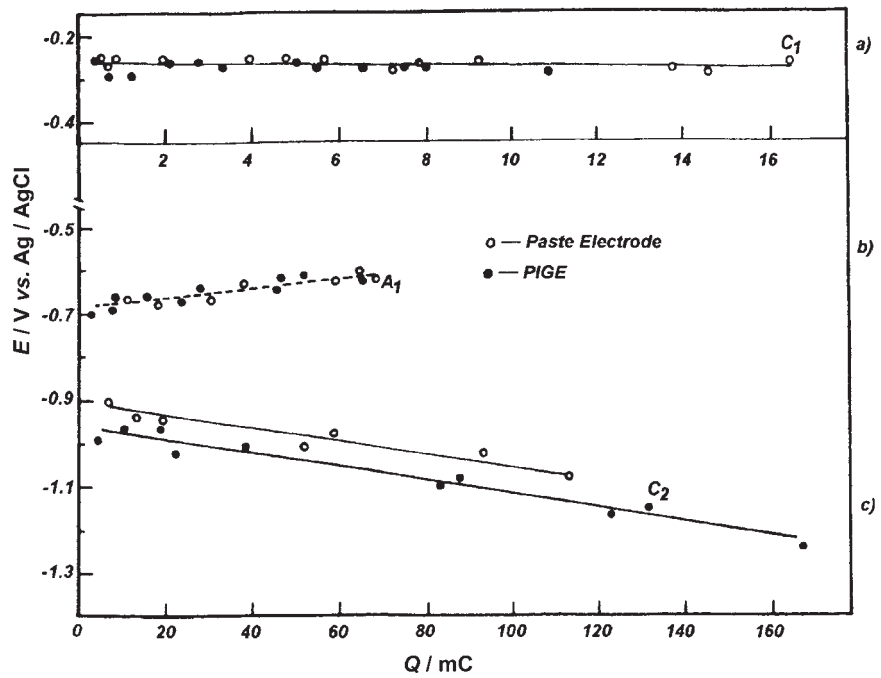

Figure 20. Plot of peak potentials *versus* the amount of consumed charge of (a) C_1, (b) A_1 and (c) C_2 for the electrochemical conversions of $BaPbO_3$ dispersed in the graphite paste electrode (–o–) and immobilized at the PIGE surface (–●–). Experimental conditions as in Figure 18.

positive potentials. For example, the difference between the peak potentials of C_2 of PbO_2 and $BaPbO_3$ will amount to 100 mV, if a graphite paste electrode is used, and to 120 mV, if a PIGE is used. A comparison of the charges of peaks C_1 and C_2 shows that, as in the case of PbO_2, only a small part (< 0.1 of it) takes part in the reaction (31). Almost all $BaPbO_3$ is reduced at peak C_2 to elementary lead, the oxidation of which is observed as peak A_1. The parameters of this oxidation process (Figures 20b and 21b) are fully identical with those, which have been observed in case of PbO and PbO_2. A comparison of the areas below peak C_2 and A_1 shows that the ratio $Q(C_2)/Q(A_1)$ is always significantly bigger than 2 for both the PIGE (2,56 ± 0.05) and the graphite paste electrode (2.35 ± 0.12). This strange re-

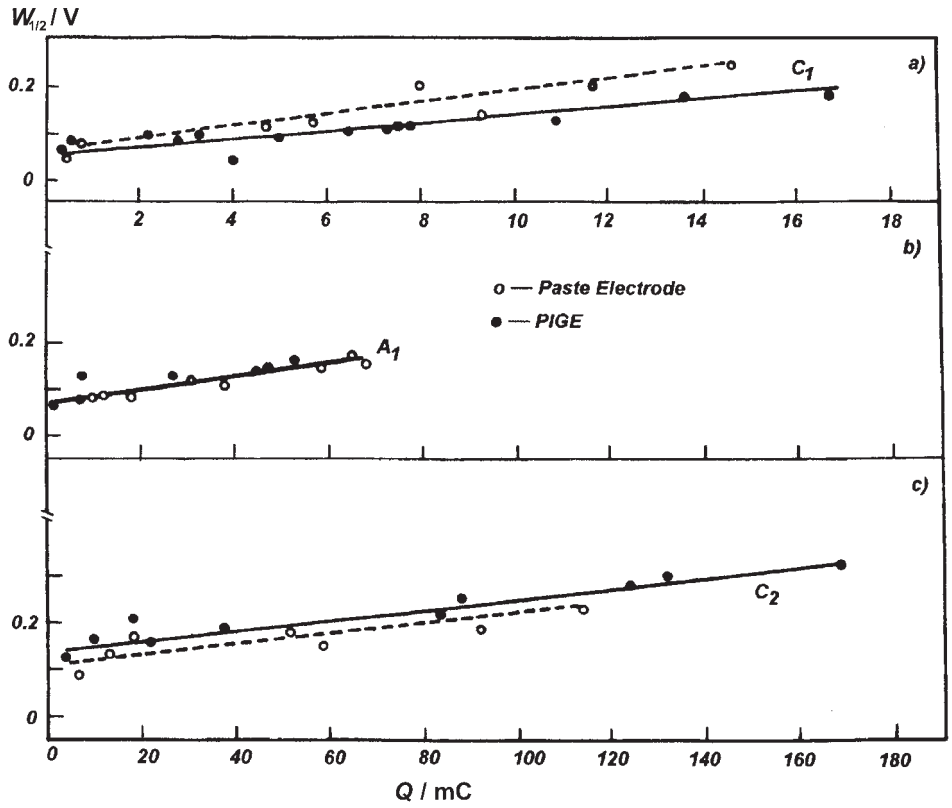

Figure 21. Plot of half-width of peaks *versus* the amount of consumed charge of (a) C_1, (b) A_1 and (c) C_2 for the electrochemical conversions of $BaPbO_3$ dispersed in the graphite paste electrode (–○–) and immobilized at the PIGE surface (–●–). Experimental conditions as in Figure 18.

sult can be understood, if we take into account that the real composition of the studied phase is $Ba_{0.8}PbO_{3.1}$ and not $BaPbO_3$:

$$Ba_{0.8}PbO_{3.1} + 1.6OH^- + 4.6e^- \rightarrow 0.8Ba(OH)_2 + Pb^o + 3.1O^{2-} \qquad (32)$$

Thus, the reduction of $Ba_{0.8}PbO_{3.1}$ requires 4.6 and not 4.0 electrons. This means that the expected ratio for $Q(C_2)/Q(A_1)$ should be 2.3, which is near to the experimental value. The observed deficit of barium and the surplus of oxygen are not unusual. On the contrary, it is very difficult to obtain a stoichiometric phase. It has been shown[36] that samples of barium metaplumbate are microheterogeneous and that the ratio of Ba/Pb changes from 0.80 to 0.97. The amount of oxygen ranges between 2.9 and 3.8. Apparently, the nonstoichiometry is the reason for the metallic conductivity, which is not typical of oxides with a perovskite structure. The specific resistance of $Ba_\varepsilon PbO_{3+\delta}$ ranges between 15–300 [36] or 200–600 μΩ cm [37] and depends on the temperature of the thermotreatment,[36] *i.e.* on the nonstoichiometry of the samples. For the oxide compound with the nonstoichiometric composition, it is typical that the holes are located at the oxygen, and it is possible that the generation of O^- takes place.[20] For our sample, the ionic composition can be given as $Ba_{0.81}Pb^{IV}_{0.43}Pb^{II}_{0.57}O^{II}_{1.38}O^{I}_{1.72}$. The presence of O^- and of Pb^{4+} and Pb^{2+} (the authors of Ref. 36 confirmed this by RFES) may be the reason for the observed shape of the voltamograms of $BaPbO_3$ (Figure 18) and for all observed experimental data. Thus, the presence of oxygen, which easily accepts electrons, may shift the reduction potentials to more positive values than for PbO or PbO_2. The peak will be narrower because the reduction is not divided into several steps as in the case of PbO_2.

CONCLUSIONS

This study was primarily aimed at elucidating the differences and similarities which are observed in the voltammetry of solid materials when they are incorporated into a graphite paste electrode and mechanically immobilized at the surface of a graphite electrode. The most striking result is that the presence of an organic binder (paraffin oil) in the paste electrodes does not inhibit the electrode processes as one could expect. The second interesting result is that the paste electrode seems to keep the educts and products of the electrode reaction so much more effectively at the electrode surface that the chemical reversibility of the voltammetric systems is better than in case of solid particles, which are immobilized at the surface of the electrode. In the latter case, the chemical and electrochemical dissolution of the small

amounts of immobilized particles result in a more pronounced loss of substance during the electrochemical transitions, most probably due to an effective diffusion of dissolved products into the adjacent solution.

Acknowledgement. – This joint German-Russian research project was generously funded by Bundesministerium für Forschung und Technologie. F. Sch. acknowledges additional support from Fonds der Chemischen Industrie. The authors express their thanks to N. G. Naumov for the synthesis of compounds and X-ray powder diffractometry.

REFERENCES

1. F. Scholz and B. Meyer, *Voltammetry of Solid Microparticles Immobilized on Electrode Surfaces* in: A. J. Bard and I. Rubinstein (Eds.), *Electroanalytical Chemistry, A Series of Advances*, Vol. 20, Marcel Dekker, Inc., New York, pp. 1998, 1–86.
2. The home page of *Voltammetry of Immobilized Microparticles*: http://www.iic.cas.cz/~grygar/AbrSV.html
3. F. Scholz and B. Meyer *Chem. Soc. Rev.* **23** (1994) 341.
4. R. E. Dueber, A. M. Bond, and P. G. Dickens, *J. Electrochem. Soc.***139** (1992) 2363.
5. A. M. Bond, R. Colton, F. Daniels, D. R. Fernando, F. Marken, Y. Nagaosa, R. F. M. Van Steveninck, and J. N. Walter *J. Am. Chem. Soc.* **115** (1993) 9556.
6. A. M. Bond and F. Marken, *J. Electroanal. Chem.* **372** (1994) 125.
7. A. Dostal, B. Meyer, F. Scholz, U. Schröder, A. M. Bond, F. Marken, and Sh. J. Shaw, *J. Phys. Chem.* **99** (1995) 2096.
8. A. Dostal, U. Schröder, and F. Scholz, *Inorg. Chem.* **34** (1995) 1711.
9. A. Dostal, G. Kauschka, S. J. Reddy, and F. Scholz, *J. Electroanal. Chem.* **406** (1996) 155.
10. Kh. Z. Brainina and E. Ya. Neyman, *Tverdofasnie reakcii v elecktroanaliticheskoj khimii,* Khimiya, Moskva, 1982, pp. 202–207.
11. Kh. Z. Brainina, E. Ya. Neyman, and V. V. Slepushkin, *Inversionnie elektroanalyticheskie metodi.* Khimiya, Moskva, 1988, p. 138.
12. Kh. Z. Brainina and E. Ya. Neyman, *Electroanalytical Stripping Methods*, J. Wiley and Sons, New York, 1993.
13. Kh. Z. Brainina and M. B. Vidrevich, *J. Electroanal. Chem.* **121** (1981) 1.
14. V. I. Belyi, T. P. Smirnova, and N. F. Zakharchuk, *Appl. Surf. Sci.* **39** (1983) 492.
15. M. Lamache and D. Bauer, *J. Electroanal. Chem.* **79** (1977) 359.
16. N. F. Zakharchuk, T. P. Smirnova, V. I. Belyi, and I. G. Yudilevich, *Rost poluprovodnikovikh krystallov i plyonok,* Part 2, Nauka, Novosibirsk, 1984, pp. 143–151.
17. B. A. Kolesov, N. F. Zakharchuk, I. G. Vasilyeva, and L. P. Kozeeva, *J. Solid State Commun.* **84** (1992) 645.
18. A. A. Kamarsin, N. F. Zakharchuk, and H. Bach, Abstracts of First German-Russian Symposium on Physics of Novel Materials, »Frankfurt Haus«, Riezlern, Kleinwalsertal, 14–16 Oct. 1993, p. 3.
19. A. G. Nemudry, N. F. Zakharchuk, and I. G. Vasilyeva, *Sverkhprovodimost` Phisika, Khimiya, Tekhnika* **68** (1993) 1446.
20. V. E. Fedorov, N. G. Naumov, N. F. Zakharchuk, N. I. Matskevich, and Paek U-Hyon, *Bull. Korean Chem. Soc.* **16** (1995) 484.

21. N. F. Zakharchuk, B. Meyer, H. Hennig, F. Scholz, A. Jaworski, and Z. Stojek, *J. Electroanal. Chem.* **398** (1995) 23.
22. N. F. Zakharchuk and N. S. Borisova, *Elektrokhimiya* **28** (1992) 1757, 1787.
23. B. Centeno, M. L. Tascon, M. D. Vazquez, and M. Sánchez-Batanero, *Electrochim. Acta* **36** (1991) 277.
24. A. J. Bard, R. Parsons, and J. Jordan, *Standard potentials in aqueous solution,* Dekker, New York, Basel, 1985, p. 220.
25. *Spravochnik po elektrokhimii,* Khimiya, Leningrad, 1981, p. 143.
26. D. Dobosh, *Elektrokhimicheskie konstanti,* Mir, Moskva, 1979, pp. 226–238.
27. V. M. Latimer, *Okislitelnie sostoyaniya elementov v vodnikh rastvorakh.* Inostrannaya Literatura, Moskva, 1954 p. 154.
28. *Encyclopedia of Electrochemistry of the Elements*, Dekker, New York, 1973, p. 1243.
29. J. P. Carr and N. A. Hampson, *Chem. Rev.* **72** (1972) 679.
30. J. P. Carr and N. A. Hampson, *J. Electrochem. Soc.* **118** (1971) 1262.
31. P. Chartier and R. Poisson, *Bull. Soc. Chim. Fr.* **7** (1969) 2255.
32. N. E. Bagshaw, R. L. Clarke, and B. Halliwell, *J. Appl. Chem.* **16** (1966) 180.
33. A. J. Bard and L. R. Faulkner, *Electrochemical Methods. Fundamentals and Applications,* J. Wiley and Sons, New York, 1980.
34. B. Meyer, B. Ziemer, and F. Scholz, *J. Electroanal. Chem.* **392** (1995) 79.
35. *Gmelins Handbuch der anorganischen Chemie,* Verlag Chemie, Vol. 47 (Blei), Teil C, Weinheim, 1969.
36. I. V. Ol'kchovik, E. D. Politova, M. V. Fedotova, S. G. Prutchenko, Y. N. Venevzev, and G. M. Kuzmicheva, *J. Neorg. Khim.* **38** (1993) 1461.
37. I. V. Ol'kchovik, E. D. Politova, S. Y. Stefanovich, and Y. V. Yurchenko, *J. Neorg. Khim.* **37** (1992) 142.

SAŽETAK

Usporedba elektrodâ od oksidâ olova u grafitnoj pasti i vezanih na čvrsti grafit

Nina Zakharchuk, Stefan Meyer, Britta Lange i Fritz Scholz

Za usporedbeno proučavanje elektroda od crvenog PbO, α-PbO_2, β-PbO_2, i $BaPbO_3$ priređenih na dva različita načina primijenjena je ciklička voltammetrija. U prvom su slučaju mikrokristalne čestice oksida olova imobilizirane na površini štapićaste grafitne elektrode impregnirane parafinom (PIGE), a u drugom su slučaju oksidi olova dodani pasti pripravljenoj od grafita i silikonskog ulja. Tako pripremljene elektrode ponašaju se slično dobro poznatim elektrodama pripravljenima od praškastih oksida olova. Također je utvrđeno da su elektrokemijske reakcije na elektrodama od paste silikona i grafita reverzibilnije nego PIGE.